Electronic Supplementary Material (ESI) for Materials Advances.

Supplementary Information

Preferential growth of perovskite $BaTiO_3$ thin films on $Gd_3Ga_5O_{12}$(100) and $Y_3Fe_5O_{12}$(100) oriented substrates by Pulsed Laser Deposition

T. Ruf[a,*)], S. Merker[b)], F. Syrowatka[c)], P. Trempler[c)], G. Schmidt[c,d)], M. Lorenz[e)], M. Grundmann[e)], R. Denecke[a)]

E-Mail: thomas.ruf@uni-leipzig.de, Tel.: +49 0341/9736457

a) Wilhelm-Ostwald-Institut für Physikalische und Theoretische Chemie, Linnéstraße 2, 04103, Leipzig, Germany
b) Institut für Anorganische Chemie, Universität Leipzig, Johannisallee 29, 04103, Leipzig, Germany
c) Interdisziplinäres Zentrum für Materialwissenschaften, Martin-Luther-Universität Halle-Wittenberg, Heinrich-Damerow-Str. 4, 06120, Halle, Germany
d) Institut für Physik, Martin-Luther-Universität Halle-Wittenberg, Von-Danckelmann-Platz 3, 06120, Halle, Germany
e) Felix-Bloch-Institut für Festkörperphysik, Universität Leipzig, Linnéstraße 5, 04103, Leipzig, Germany

* corresponding author

Supplementary texture coefficients

To provide complementary information on texture coefficients of BTO thin films corresponding to Figure 1 in the main text, Table S 1 lists further values for the GGG(110) and GGG(111) substrates. As BTO(201) cannot be included for BTO thin films on GGG(111), the texture coefficients add up to 4 for the thin films on the latter substrates. For comparison, samples on GGG(100) or YIG(100) with deposition temperature ≥ 755 °C show TC(110) values above 3.8 and simultaneously exhibiting a multiple in absolute intensity for the BTO(110) reflex.

Table S 1: Calculated texture coefficients for the BTO(110), BTO(200) and BTO(111) orientations for BTO thin films on GGG and YIG substrates of different orientations and processing conditions. Because of low signal-to-noise ratios for some samples in general and in others for minor intensity reflexes, the texture coefficients should be read with a relative error of 25 %. The intensity was determined by fitting Gaussian functions for simplification. As the following groups of reflexes could not be resolved, the BTO(110) and BTO(101) were summarized to BTO(110), the BTO(201), BTO(120) and BTO(102) was incorporated into BTO(201) and BTO(211) comprises BTO(211) and BTO(112), as well as BTO(200) and BTO(002) assigned as BTO(200). Texture coefficients on GGG(111) substrate do not include the BTO(201) reflex, since the latter is overlapped by the GGG(444) substrate reflex. The values for TC(201) and TC(211) are mostly around 1 or lower and are left out.

Substrate and procedure	TC(110)	TC(200)	TC(111)
GGG(111), 700 °C	0.9	1.1	1.0
GGG(111), 755 °C	1.0	0.9	1.1
GGG(111), 755 °C, s.l.	1.1	1.6	0.7
GGG(111), 800 °C, s.l.	1.8	1.6	0.3
GGG(110), 755 °C, s.l	1.5	1.1	1.9
GGG(110), 800 °C, s.l.	2.0	1.6	0.0
YIG(111)/GGG(111), 700 °C	1.1	0.8	0.9

XPS heating study on a BTO thin film

In Figure S 1, the O 1s and Ba $3d_{5/2}$ detail spectra of a BTO thin film on Nb:$SrTiO_3$(100) after heating in UHV are shown. Heating to 475 °C leads to an increase in the O 1s signal for Bulk BTO at 529.1 ± 0.1 eV and a small enhancement of the Ba $3d_{5/2}$ at 778.3 ± 0.1 eV (Table S 2). Also, after heating to 475 °C, the C 1s detail spectra (not shown here) does not show any carbonate signal around 288.6 eV anymore. These measurements suggest, that the high-binding energy components in O 1s and Ba $3d_{5/2}$ detail spectra are to be related majorily to surface phases and not only contaminations, such as $Ba(OH)_2$ or $BaCO_3$.

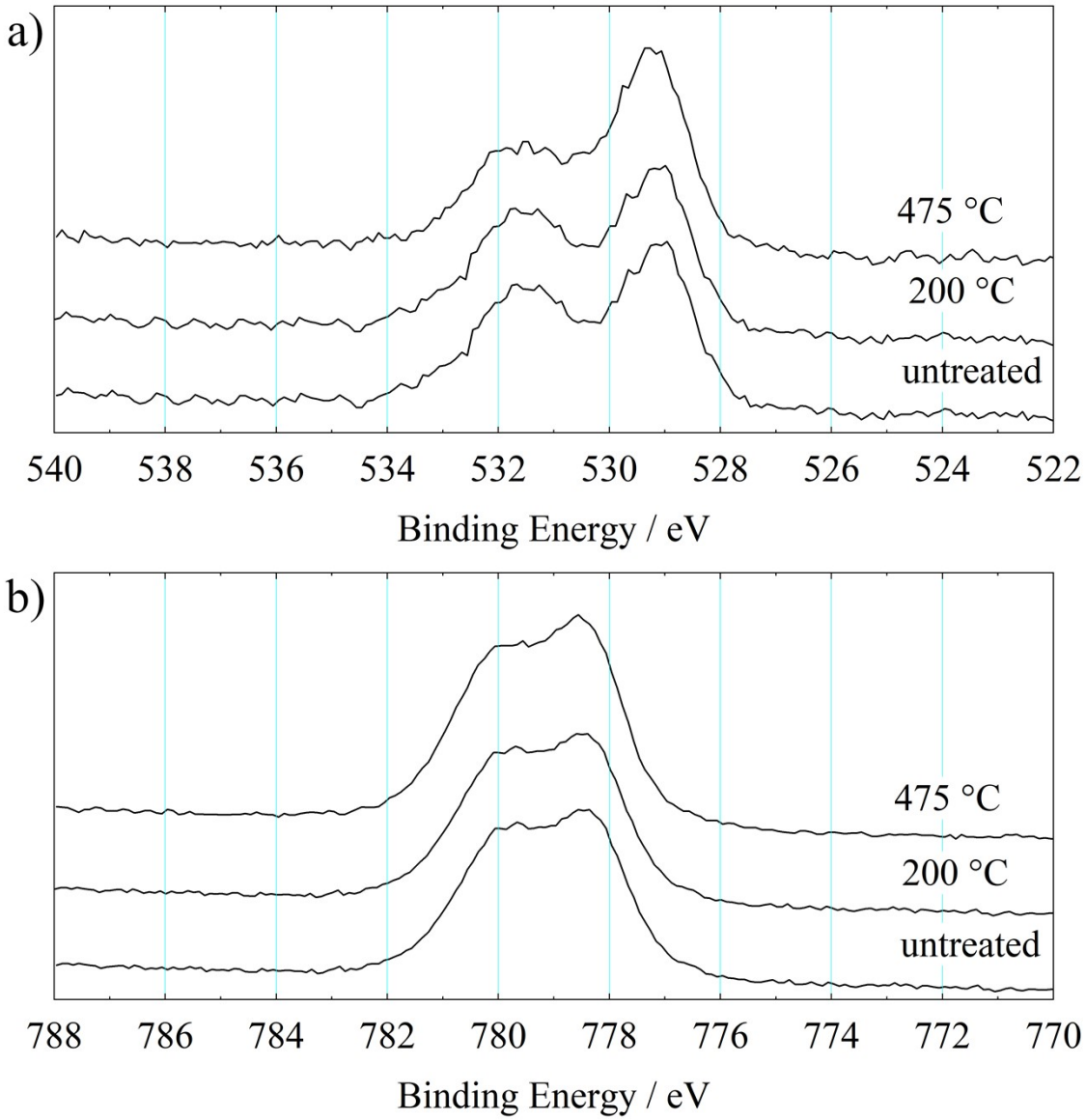

Figure S 1: Comparative detail spectra after heating in UHV of O 1s (a) and Ba $3d_{5/2}$ (b) of a 500 nm BTO thin film deposited at 700 °C on a Nb:$SrTiO_3$ (100) substrate. A constant background was subtracted from the detail spectra, which corresponds to the intensity at the low binding energy side. The heating steps at 200 °C and 475 °C were held for 30 min respectively and then the sample measured after cooling to room temperature without removing from the UHV chamber.

Table S 2: Heating study of a BTO thin film deposited on Nb:$SrTiO_3$(100). Binding energies in eV of O 1s and Ba $3d_{5/2}$ and relative quantitative part of the respective photoelectron line is given in parenthesis in per cent.

samples	untreated	Heated to 200 °C	Heated to 475 °C
E_B(O1s)	529.1(48.2)/531.2(33.3) /532.3(18.5)	529.2(53.1)/531.2(27.1) /532.1(19.7)	529.2(59.4)/531.3(17.2) /532.4(23.4)
E_B (Ba $3d_{5/2}$)	778.3(54.4)/780.0(45.6)	778.4(54.7)/780.1(45.3)	778.4(56.3)/780.1(43.7)

XPS investigation of BTO thin films deposited at temperatures at and above 755 °

For discussion of the apparently high concentration of Bi in XPS quantification of samples processed at 755 °C or higher, please refer to the main text. In this part of the supplementary files no detail spectra of Ba 3d, Ti 2p, O 1s or Bi 4f are shown, since they resemble closely those depicted in Figure 2 and Figure 3 in the main text. Here some remarks about the relative quantification within these samples, that have a Bi/Bi-oxide surface contamination shall be added:

- Stoichiometric ratios of oxygen to Ba and Ti are affected, as the corresponding O 1s signal of Bi_2O_3 (literature values: 529.9 eV [1] and 530.4 eV [2]) and possibly $Bi(OH)_3$ contribute at similar binding energies as O 1s of BTO. E.g. the ratios $[O_{529eV}]/[Ti]$ and $[O_{531eV}]/[Ba_{780eV}]$ are overestimated.
- Photoelectron lines of different kinetic energies are diversely attenuated by the Bi/Bi-oxide structures on the surface. So the Ba 3d line should be more affected than the Ba 4d line.
- The Bi $4d_{3/2}$ photoelectron line is situated close to the Ti $2p_{1/2}$. Although only Ti $2p_{3/2}$ is evaluated, the background estimation of this area is complicated.

However, especially the binding energy values for the components in Ba $3d_{5/2}$, O 1s and Ti $2p_{3/2}$ are still in accordance with the values for BTO cited or reported in the main text. Due to the above described reasons, the deviations in stoichiometric results to nominal composition are deemed acceptable.

Table S 3: XPS binding energies in eV and XPS quantifications, in part differentiated in components, of BTO films deposited at 755 and 800°C on different GGG substrates. In parenthesis after the binding energies the relative quantitative part of the respective orbital in per cent is denoted. For quantification of Bi relative to other elements, the Ba 4d detail spectrum was used. The at.%(C) consists of the so-called adventitious hydrocarbon, the carbonaceous impurity on all ex-situ samples.

Sample	BTO on GGG(100) s.l., 755 °C, 200 nm	BTO on GGG(111) s.l., 755 °C, 200 nm	BTO on GGG(100) s.l., 800 °C, 200 nm
E_B(O 1s)	529.3(72.8)/530.6(12.5)/ 531.7(14.7)	529.4(79.8)/531.1(15.9)/ 532.3(4.3)	529.2(71,5)/530.5(12.7)/ 531.6(15.7)
E_B(Ba $3d_{5/2}$)	778.7(80.7)/780.2(19.3)	778.7(81.6)/780.2(18.4)	778.5(83.4)/780.0(16.6)
E_B(Ba $4d_{5/2}$)	88.2(85.9)/89.6(14.1)	88.3(87.7)/89.7(12.4)	88.0(89.5)/89.2(10.6)
E_B(Ti $2p_{3/2}$)	458.1	458.1	457.9
[Bi]/([Bi]+[Ba]+[Ti])	14.9 %	14.0 %	16.9 %
[Bi]/([Ba]+[Ti]+[O])	6.8 %	6.8 %	7.6 %
[Bi](metal)/ ([Bi](metal)+[Bi](Bi_2O_3))	14.5 %	32.8 %	6.0 %
[Ba_{778eV}]/[Ti]	1.5	1.3	1.4
[O_{529eV}]/[Ti]	3.6	3.4	4.0
[O_{529eV}]/[Ba_{778eV}]	2.4	2.5	2.8
[O_{531eV}]/[Ba_{780eV}]	3.8	2.9	5.5
at.%(C)	22.3	29.5	33.2

XPS sputter study on a BTO thin film deposited at 755 °C on GGG(100)

In Figure S 2 a sputter study of a 200 nm BTO thin film deposited on GGG(100) at 755 °C is shown. These survey spectra are measured with an excitation energy of 1253.6 eV (Mg-K_{alpha}), which provides even higher surface sensitivity compared to Al-excitation. Sputtering with 1 keV Ar^+-ions removes the initially high surface aliphatic hydrocarbon (see C 1s), as well as Bi as observed in diminishing Bi 4f and Bi 4d photoelectron lines. The decrease of measured surface concentration of Bi is then caused by a higher intensity of Ba, O and Ti lines through removing carbonaceous and Bi surface contaminations and eventually by a lower intensity of the Bi photoelectron lines themselves. This further proves, that Bi is situated at the surface of the thin films. A full removal of Bi contamination is not possible, since the surface roughness of approx. 5 nm (RMS value) effects shadowing.

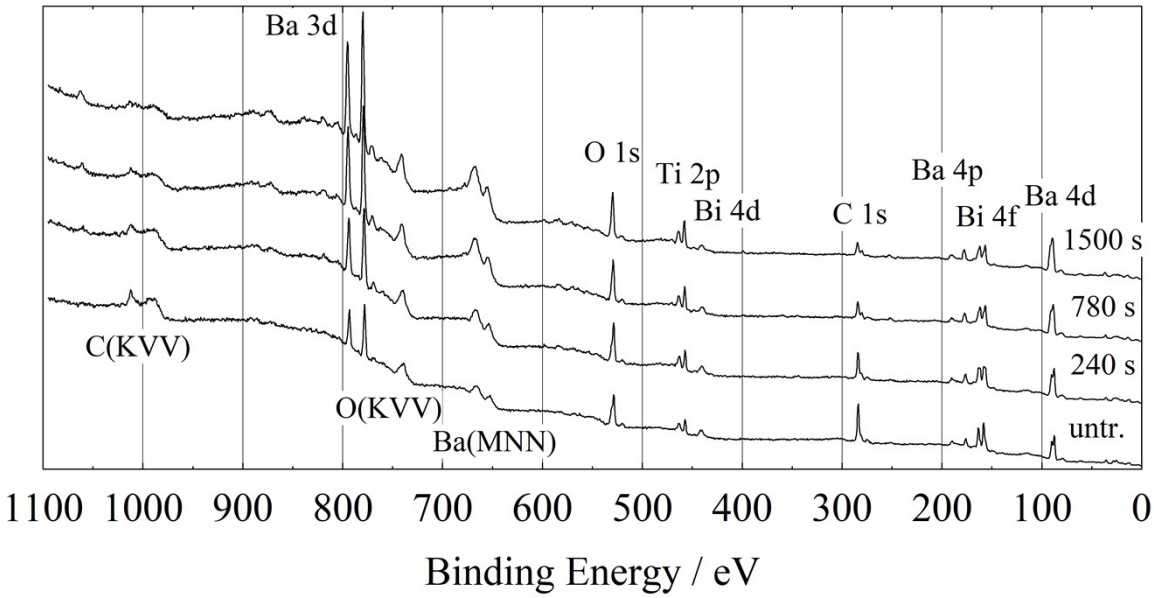

Figure S 2: XPS Survey scans of a sputter study (Ar^+-ions, 1 keV) on a BTO thin film deposited at 755 °C on GGG(100). The duration of sputtering is indicated at the right.

In-plane epitaxial relationships probed by phi-scans

To check for in-plane epitaxy, phi-scans with asymmetrical reflexes, namely BTO(400), GGG(888) and YIG(842), have been performed. In case of not using a seeding layer (Figure S 3 (a)), a moderate "rectangle-on-cube" epitaxy with the edges aligned is observed. Here, the rectangle refers to the symmetry of the BTO(110) planes. A two domain growth of the BTO(110) films exhibits a four-fold symmetry in the phi-scan of the asymmetric BTO(400) reflex. This results in large in-plane lattice mismatches of 2.6 % for BTO<001>∥YIG<001> and 8.6 % for BTO<110>∥YIG<010> (Table S 4). To relieve the strain, forming a seeding layer or higher Bi surface contamination promote broader and more diffuse signals in the phi-scans (Figure S 3 (b)). That could mean that a continuum of different in-plane relationships applies in this case and promotes a relief of the strain, as exemplified for two configurations other than the edge-aligned version in Figure S 3 (d). An intermediate case shows the sample grown on YIG(100) with low at.%(Bi) in Figure S 3 (c), even if a seeding layer was used. In the latter, the epitaxy is both characterised by edge-alignment and the broader reflexes indicating a plethora of in-plane relationships. This suggests, that less Bi surface contamination and/or not using a seeding layer favours strained BTO(110) films with edge-aligned in-plane epitaxy.

Table S 4*:* In-plane epitaxial relationships as determined by ϕ-scans of asymmetrical reflexes of both layer and substrate for edge-alignment ("45 °") and two exemplary configurations for broader, diffuse reflexes ("25.5 ° and 9.7 °"). The nominal in-plane lattice mismatches are equally valid for GGG. The mismatches are calculated according to $(a_{YIG}-a_{BTO})/(a_{YIG})$, in which a_{BTO} is the interplanar distance for the corresponding miller indices.

Δϕ (BTO(400)/GGG(888) or BTO(400)/center of YIG(842))	In-plane epitaxial relationship and nominal in-plane lattice mismatches in parenthesis	Visual interpretation of the rectangle on the cube
45 °	BTO<001> ‖ YIG<010> (2.6 %), BTO<110> ‖ YIG<001> (8.6 %)	Edges aligned
~ 25.5 °	BTO<221> ‖ YIG<010> (3.0 %), BTO<114> ‖ YIG<001> (0.5 %)	turned by 19.5 °
~ 9.7 °	BTO<111> ‖ YIG<010> (6.6 %) BTO<112> ‖ YIG<001>(- 5.9 %)	turned by 35.3 °

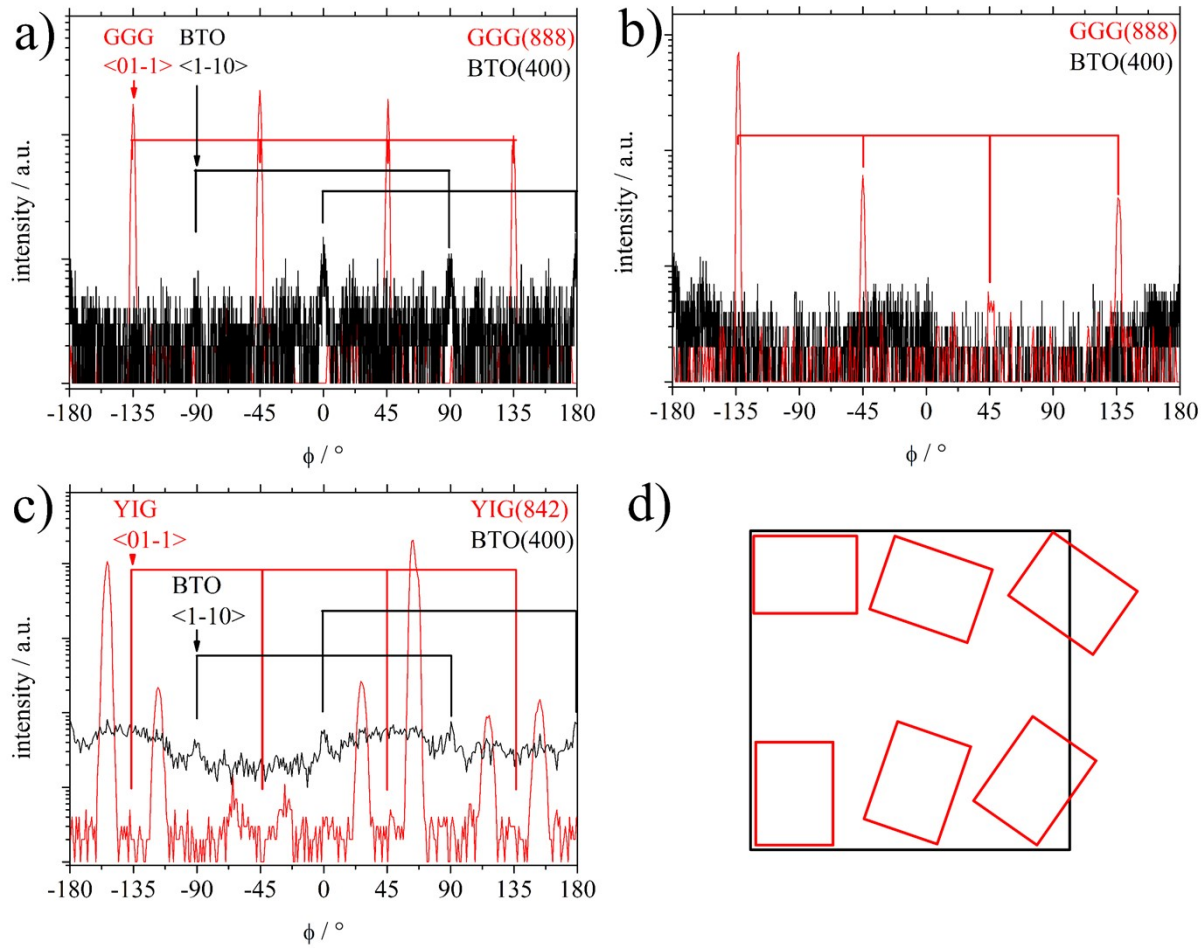

Figure S 3: Phi-scans of asymmetrical reflexes GGG(888) and BTO(400) for a 200 nm BTO thin film on GGG(100) deposited at 755 °C (a), phi-scan of asymmetrical reflexes GGG(888) and BTO(400) for a 500 nm BTO thin film on GGG(100) deposited at 755 °C and applying a seeding layer (b) and a phi-scan with asymmetrical reflexes YIG(842) and BTO(400) deposited at 755 °C and a seeding layer (low at.%(Bi)) (c). The lines are added for indication of a set of reflexes in the phi-scan. In (a,c) in-plane directions are indicated. Schematic interpretation of the rectangle-on-cube epitaxy as applying to edge-aligned and with an off-set of 19 and 35 ° (d) for exemplification of deviating in-plane epitaxial relationships.

1 K. Uchida, A. Ayame, Surf. Sci. 357-358 (1996) 170.

2 V.S. Dharmadhikari, S.R. Sainkar, S. Badrinarayan, A. Goswami, J. Electron Spectrosc. Relat. Phenom. 25, (1982) 181.